The Effect of Bandgap Grading on Performance on Lead-Free Perovskite Solar Cells

Nor Azlian Binti Abdul Manaf[1], Corresponding Author[1,*], Wan Yusmawati Binti Wan Yusof[1], Azuraida Binti Amat[1] and Asyraf Hakimi Bin Azmi[1]

[1] Physics Department, National Defence University of Malaysia, Kem Sungai Besi, 57000 Kuala Lumpur, Malaysia

ARTICLE INFO

Article history:
Received
Received in revised form
Accepted
Available online

Keywords:

Minimum three keywords; Graded Bandgap; Lead-Free Perovskite Solar Cells

ABSTRACT

Lead (Pb)-halide perovskite materials have been widely used in perovskite solar cells (PSCs) application but the presence of Pb in this device can harm human beings and environmental to a significant extent. Thus, the search toward Pb-free-halide perovskite and low-toxicity materials has been done to replace the conventional Pb-halide perovskite for sustainable environment. Among the possible Pb-substitution strategies, the trivalent bismuth (Bi) cation possesses the same electronic configuration as Pb and comparable optoelectronic properties to the Pb-halide perovskites. Unfortunately, Bi-halide PSCs showed a very small power conversion efficiency (PCE) compared to Pb-halide PSCs. This work demonstrated how the device architecture able to overcome the efficiency related challenge in PSCs. The graded bandgap structure has been designed in Bi-halide PSCs to improve the output current and PCE by maximizing the solar spectrum. In this work, Titanium dioxide (TiO_2) was used as electron transport layer (ETL) and Spiro-OMeTAD was used as hole transport layer (HTL) due to its facile implementation and high performance in electronic device. The variation of ioidine concentration in Bi-doped iodide estabishes bandgap tuning and conductivity type of the layer. The increse of iodine concentration would reduce band gaps and induce the change of semiconductor behavior from n-type to p-type. In this strategy, the absorbance component consists of three Bi-based perovskite layer with different concentration of iodine that form n- and p- type homojuctions. This configuration produces cells with desirable perforamance that effectively absorb the photons in almost all parts of the solar spectrum. The open circuit voltage (V_{oc}) (940 mV), short current densities (J_{sc}) (~25 $mAcm^{-2}$) and fill factors (~58%) for the best cells have shown drastic improvement compared to single active layer device. The effects of quasi-electric fields due to the band-gap variation of the active semiconductor, upon the illumination J_{sc} and V_{oc} will be discussed further.

* *Corresponding author.*
E-mail address: azlian@upnm.edu.my

1. Introduction

Perovskite materials Lead (Pb) halide perovskite solar cells have shown a rapid development in power conversion efficiency (PCE) due to the excellent characteristics such as high light absorption coefficients, low temperature solution processing capability, narrow band emission, direct bandgaps, long exciton diffusion lengths, suitable charge carrier lifetimes, high photoluminescence quantum yields and low nonradiative carrier recombination rates. However, lead (Pb) is recorded by the World Health Organization as a pollutant and chemical known to caused birth defect and cancer along with environmental concern, and its usage is restricted under several international legislations. Therefore, it is imperative to explore Pb-free perovskite materials for PSCs for a sustainable and safe environment. Multiple studies have documented findings to use lead-free materials to replace the Pb in perovskite solar cells without negatively affecting their performance. The general formula of Pb perovskite is $APbX_3$, where A is the monovalent cation and X is the halogen anion. To replace the Pb^{2+} cations, the employment of other divalent metal cations such as Sn^{2+} or Ge^{2+} should be utilized to maintain the charge neutrality. Another approach is by replacing the two Pb^{2+} cations with a monovalent cation (Ag^{+}) and a trivalent cation (Bi^{3+}). The crystal structure of this kind of perovskite named as double perovskite since the unit cell is double that of ABX_3 Pb-halide perovskite [1]. The double perovskite maintains the 3-dimension ABX_3 perovskite structure. However, it exhibits a wide bandgap, large exciton binding energy, low carrier mobility and poor charge transport ability. Due to these limitations, the PCEs of lead-free based PSCs are around 3–4 % [2,3].

The key issues concern now is how to achieve further improvements in efficiency for lead-free PSCs. Perovskite solar cells (PSCs) are traditionally fabricated in a single bandgap device structure where an active layer, lead-halide is deposited in between of hole-transport layer (HTL) and electron-transport layer (ETL). This mechanism enables conventional device structures to be able to surpass efficiency of ~20% for Pb-halide PSCs and ~3-4% for lead-free PSCs. Research on graded bandgap perovskite has been approached to enhance the performance of the solar cell device by changing halide anion concentration and bandgap. Huq et. al tuning of the perovskite absorber layer that deposited in between gallium nitride (GaN) as an ETL and graphene aerogel as an HTL. This structure produces stable and reproducible solar cells, but the power conversion efficiency (PCE) is still low [4]. Another work on multi-junction tandem cells has been done using a tunable bandgap of methylammonium-lead-halide integrated with crystalline silicon and copper indium gallium selenide (CIGS) [5,6]. However, it necessitates interconnection between the perovskite sub-cells and complicated electrical coupling, which causes electron-hole recombination centers.

Here, we proposed good efficiency of graded bandgap lead-free perovskite solar cells heat treated at optimum temperature based on the prior Bi-halide perovskite thin film characterization. A range of different bandgaps is obtained by compositional engineering of ABX_3 perovskite semiconductors, where methylammonium (MA) is commonly utilized as monovalent A-cations within the perovskite lattice. The increse of iodine concentration in bismuth halide ($MA_3Bi_2I_9$) would reduce band gaps and induce the change of semiconductor behavior from n-type to p-type [7]. In this strategy, the absorbance component consists of three Bi-based perovskite layer with different concentration of iodine that form n- and p- type homojuctions. This structure enables wide absorption of the spectrum, lead to a higher J_{sc} value and resulting in efficiency beyond the Shockley-Queisser limit (SQL).

2. Methodology

2.1 Thin film preparation and characterization

Bismuth (Bi) halide perovskite thin film was deposited using modified successive ionic layer adsorption and reaction (SILAR) technique. To start the synthesization of the solution, two beakers, with each contained 50 ml of deionized water were prepared as shown in Figure 1. The first beaker was added with 0.5 M of bismuth (III) nitrate ($Bi(NO_3)$) while another beaker was added with 0.5 M potassium iodide (KI). Both solutions were stirred for 30 minutes. The third beaker contained deionized water was prepared as the rinse bath. Glass/ITO substrate was used as substrate in this work. It was clean thoroughly before the coating process. The coating process started with initially dipped the glass/ITO into the first beaker for 10 s and straight dipped to the second beaker for chemical reaction for 20 s. Finally, the glass/ITO was dipped in the third beaker and rinsed to complete one cycle dipping process. During the dipping process, the substrate was positioned inclined in the beaker. The dipping cycle process was repeated for 30 times to obtained a decent layer. The deposited Bi-halide perovskite layers were heat treated at various temperature starting from 250°, 350°, 450° and 550° C. The thickness, microstructural and electrical conductivity of Bi-halide films have been studied through optical profilometry, SEM, and four-probe hall effect measurement, respectively.

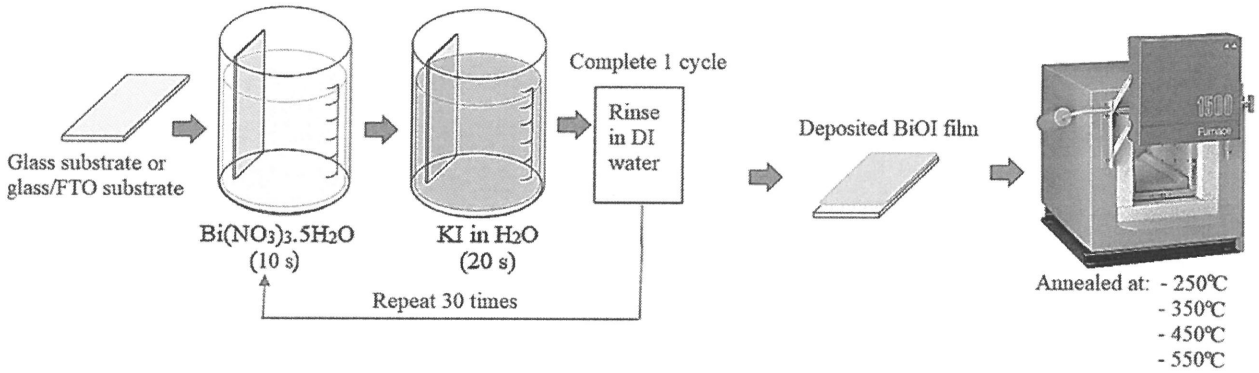

Fig. 1. Thin film deposition using SILAR dip coating technique and heat treatment process.

2.2 PSCs fabrication

The optimum layer of Bi halide was then applied as an active layer in PSCs with the device structure glass/ITO/TiO_2/Bi-halide perovskite/spiro-OMeTAD/Au. Figure 2 shows the schematic of the fabricated Bi-halide perovskite lead-free perovskite solar cells with single active layer and graded band-gap active layer. As for single active layer solar cell consists of intrinsic Bi-halide layer with bandgap of 1.66 eV is placed in between of n-type of TiO_2 as an electron transport layer (ETL) and p-type of spiro-OMeTAD as hole transport layer (HTL). As for graded bandgap active layers solar cell, the variation of ioidine concentration in bismuth-halide establish bandgap tuning and conductivity type of the three active layers fabricated in between of ETL and HTL. The device consist of TiO_2 thin film as an ETL layer deposited on a glass/ITO substrate followed by three layers of Bi-halide perovskite with different concentrations ration of iodine to bismuth. Bi-halide perovskite layer with half concentration ratio of iodine to bismuth (I:Bi = 0.5:1.0) named as Bi-halide 0.5 is deposited as first perovskite layer. The second perovskite layer comprises the $MA_3Bi_2I_9$ layer with an equal concentration ratio of iodine to bismuth (I: Bi = 1.0: 1.0) named Bi-halide 1.0. Finally, the third perovskite layer is $MA_3Bi_2I_9$ with a double concentration ratio of iodine to bismuth (I: Bi = 2.0: 1.0), named iodine Bi-halide 2.0. The increse of iodine concentration would reduce band gaps and induce

the change of semiconductor behavior from n-type to p-type in active layers layer. The HTL consists of a spiro-OMeTAD was grown using spin coating followed by the top electrode comprises a layer of gold (Au). The fabricated device was measured using I-V measurement under a solar spectrum simulator with AM 1.5 illuminations.

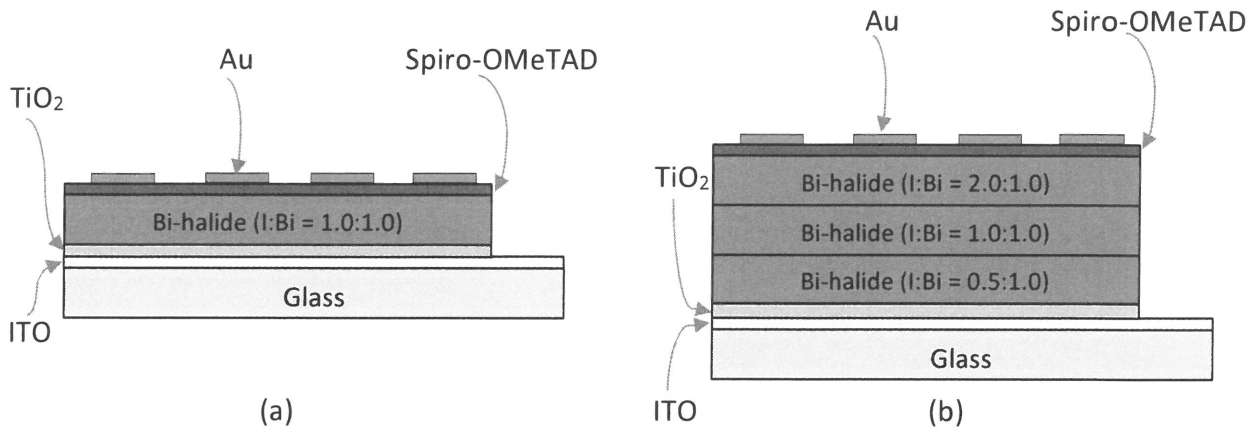

Fig. 2.: PSCs device with (a) single absorbance layer and (b) graded band-gap absorbance layer

3. Results

3.1 Bi halide characterization

Bi-halide thin films have successfully grown by SILAR techniques and these layers demonstrated good adhesion to the glass substrate as shown in Figure 3. The as-deposited Bi-halide thin film is dark orange in color. After annealing at 250 and 350°C, the color of thin film changed to orange-yellowish color. The color transformed to the pale yellow with higher annealing temperature, subsequently demonstrated a minor peel off after annealed at 550°C, thus indicated the film cannot have survived in further harsh condition than this if annealed ≥550°C.

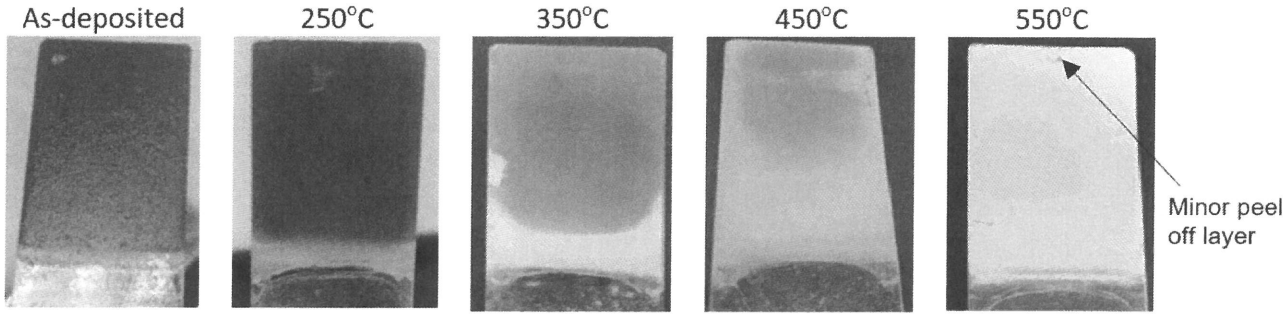

Fig. 3.: The physical observation of Bi-halide thin film for as-deposited and annealed at 350, 400, 450 and 550°C.

The thicknesses of Bi-halide thin films were characterized using optical profilometry and shown in Table 1. The thickness of as-deposited Bi-halide film is ~5.66 μm and it increased to 8.802 μm after annealed at 250°C, but reduced slightly to 7.98 μm at 350°C, that indicate the micro and macro structural features such as density, porosity and crystalline morphology improved with appropriate annealing temperature. However, the thickness decreased to ~6.51 μm as the annealing temperature greater than 450°C. The thickness of Bi-halide film demonstrated rapid decline to almost half of the

thickness (~3.48 μm) when it annealed at 550°C, thus caused by shrinkage and densification of the thin films as the result of the particles aggregation and grains coalescence.

It is suggested that the annealing process could reduce the dislocation density and strain value, hence improve the crystallinity of the film. The advantage of decrease in dislocation density is it can increase in the electrical conductivity of the films. Likewise, during annealing, materials will transform into more ordered phase and reduce defect states in the forbidden band gap. However, the appropriate annealing temperature should be considered in this study since the too high annealing temperature could cause change the dimensional due to shrinkage, hence reduced the film thickness and material deterioration. The average resistance of FTO/Bi-halide/Au structures were measured using I-V characteristics. The electrical conductivity was calculated with known thicknesses of the Bi-halide layer. Table 1 shows the measurements of average resistance, resistivity and conductivity of Bi-halide thin films as a function of the annealing temperature. It is observed that the electrical conductivity of Bi-halide film decreased slightly as it was annealed at 250°C compared to the as-deposited layer. The conductivity increased from 2.68×10^{6} to 1.63×10^{4} Sm^{-1} and achieved the highest peak after annealed at 350°C. The conductivity enhancement is due to the improvement of crystallinity, the enlargement of the flakes size and the reduction of defects which promote the higher mobility of electrons [8,9].

Table 1: The summary of thickness and electrical properties of Bi-halide thin films annealed at different temperatures.

Annealing Temperature (°C)	Thickness (μm)	Average Resistance (Ω)	Resistivity, ρ x 10^{5} (Ωcm)	Conductivity, σ x 10^{-6} Sm^{-1}
As-deposited	5.66	2.84×10^{4}	2.50	3.99
250	8.08	6.56×10^{4}	3.73	2.68
350	7.98	9.61×10^{2}	0.06	163.23
450	6.51	3.07×10^{7}	2364	0.04
550	3.48	1.50×10^{6}	216	0.46

The SEM Images of Bi halide thin films are shown in Figure 4. The as-deposited Bi-halide film consists of agglomerations of flakes with flower shape and due to that, the electrons suffer grain boundary scattering when traveling in both directions, parallel and vertical to the substrate. Therefore, the measured conductivity is low. During annealing process, these agglomerations and smaller flakes increase from ~0.8 μm to ~3.2 μm after annealed at 350°C as shown by the SEM images in Figure 4(c). Thus, the electrons can move along the fully crystalline grains from the FTO to Au contacts and there are no grain boundaries to hinder the charge carrier movements. This shows the benefits of having micro-size columnar type flakes in solar cell. The advantages of having micro size flakes or columnar in the active layer of solar cells device also have been reported earlier [10,11]. In addition to this high conductivity, the larger flakes microstructure introduces active PV junction along the grain boundaries due to melting and diffusion of doped into Bi-halide materials. The combination of these vertical junctions at the boundaries together with the main rectifying junction leads to transfer of electrons and holes in different paths and minimize the recombination. This will provide the future research direction for producing high efficiency solar cells.

However, a decreased in conductivity was observed for the Bi-halide films at annealing temperatures ≥450°C. This is probably due to the material breakdown, oxidation, sublimation of the layer at higher annealing temperature and diffusion of Na from glass to Bi-halide layer. This trend is also consistent with the thickness measurement which demonstrates the loss of material, hence reduced Bi-halide thickness after annealed ≥450°C (Figure 4(d) and 4(e)) that display the shattered

flakes microstructure for sample annealed at 550°C. Also, many have reported that the diffusion coefficient of Bi depends on several factors such as its composition, impurities, annealing temperature, time and environment [12-13]. With this observation we believed that heat treatment temperature above 450°C is closed to the activation enthalpy point for bismuth out-diffusion.

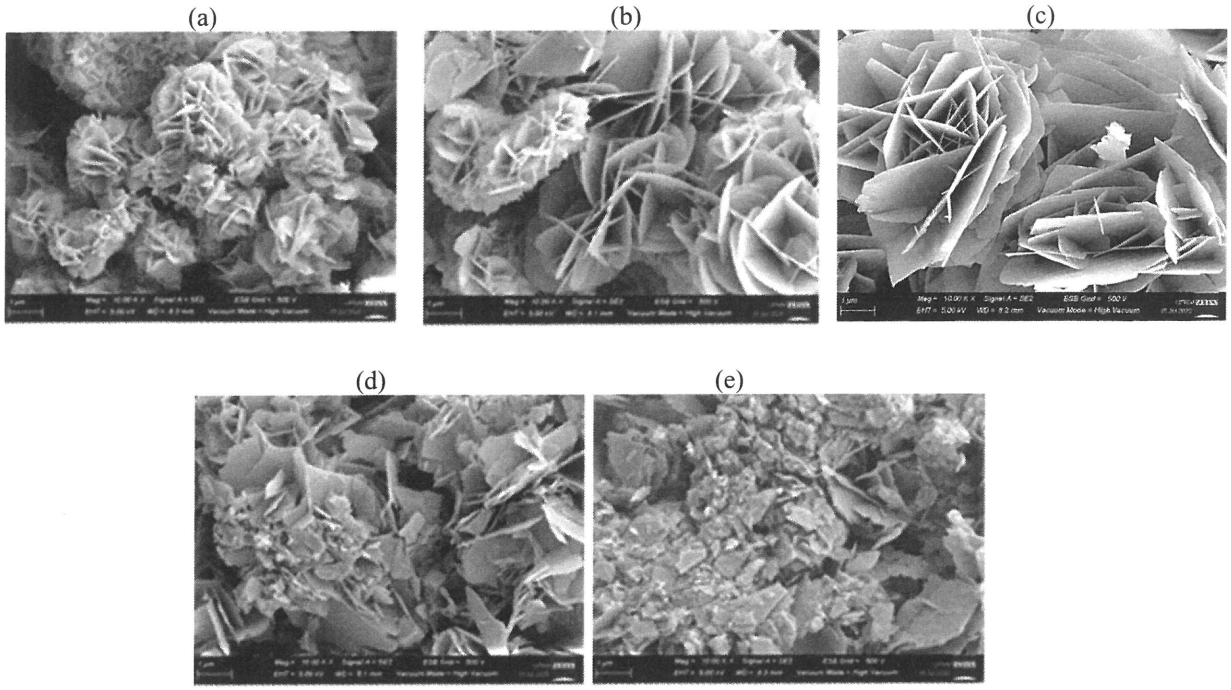

Fig. 4: The SEM Images of Bi halide thin films for (a) as-deposited and annealed at (b) 250, (c) 350, (d) 450 and (e) 550°C.

3.1 PSCs measurement

From Figure 5, it is observed that the PSCs with single active layer was measured with low J_{sc}, V_{oc} and efficiency whereas the PSCs with graded bandgap n-i-p active layers (b) was measured with good current density, J_{sc}, open circuit voltage, V_{oc} and efficiency, η with ~28.3 mAcm^{-2}, ~0.66 V and ~7.72%, respectively. This is due to the device structure with wide bandgap in the front and three perovskite layers that formed n-i-p grading structure created strong built-in electric field that speeds up the photo generated electron. The device architecture that designed bandgap tuning and conductivity type of Bi-halide films that slowly change from n-type to p-type SC (variation of iodine concentration in bismuth halide) form n- and p- type homo-juctions is so novel since it provides effective built-in electric field, the wider n-type place in front device effectively absorbs the photons in almost all parts of the solar spectrum and produces cells with desirable performance [14].

From Fig 6, it is observed that the PSCs with single active layer (a) was measured with low J_{sc}, V_{oc} and efficiency. A solar cell with a single junction can only convert a certain wavelength with highest efficiency relating to the band-gap. In fact, the thoretical limit for power conversion efficiency (PCE) on single junction solar cell is only about 20% [15]. The PSCs with graded band-gap n-i-p active layers (b) was measured with good current density, J_{sc}, open circuit voltage, V_{oc} and efficiency, η with ~28.3 mAcm^{-2}, ~0.66 V and ~7.72%, respectively. This is due to the device structure with the wider n-type layer placed in front device effectively absorbs the photons and more energy from the solar spectrum

leading to increase the photoinduced charge separation and electron transfer processes [16,17]. In addition, the band-gap tuning through three perovskite active layers that slowly change from n-type to p-type (variation of iodine concentration in bismuth halide) is so novel since it provides effective quasi-electric field to speed up drift diffusion length and enhanced carrier collection [18-19]. The quasi-electric field associated to a graded band-gap active layers in lead-free PSCs structure had better instigate both reduced bulk and surface recombination, if the field is in the appropriate direction. In this design, the band-gap reduced towards the back contact device and the required quasi-electric field should be directed towards the front contact so that electrons are drifted in the shortest direction [20]. The effects due to the associated quasi-electric field will consequently improving the open circuit voltage and current density of the device simultaneously reduce the recombination at the back contact [18-20].

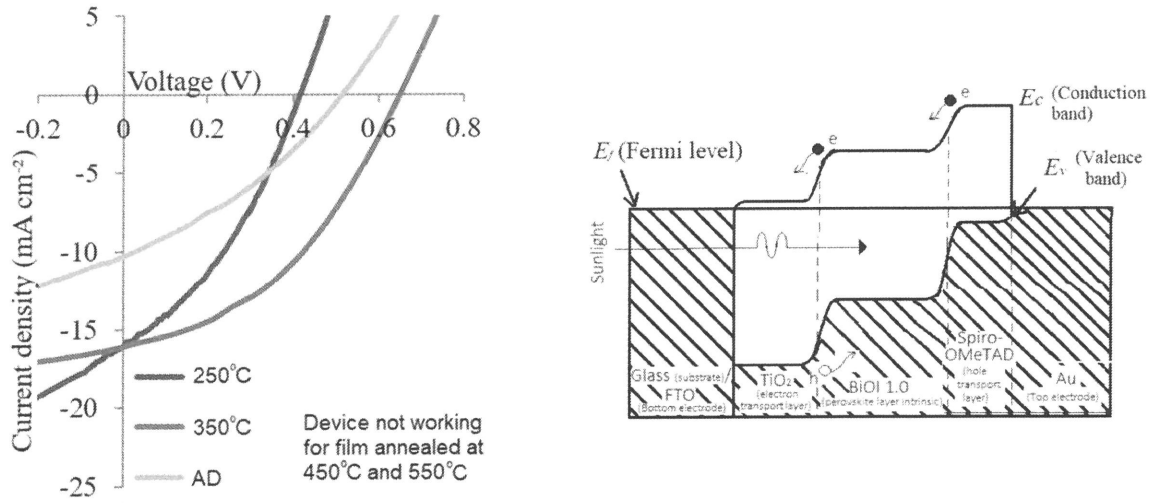

Fig. 5. J-V characteristic of a single active layer perovskite solar cell.

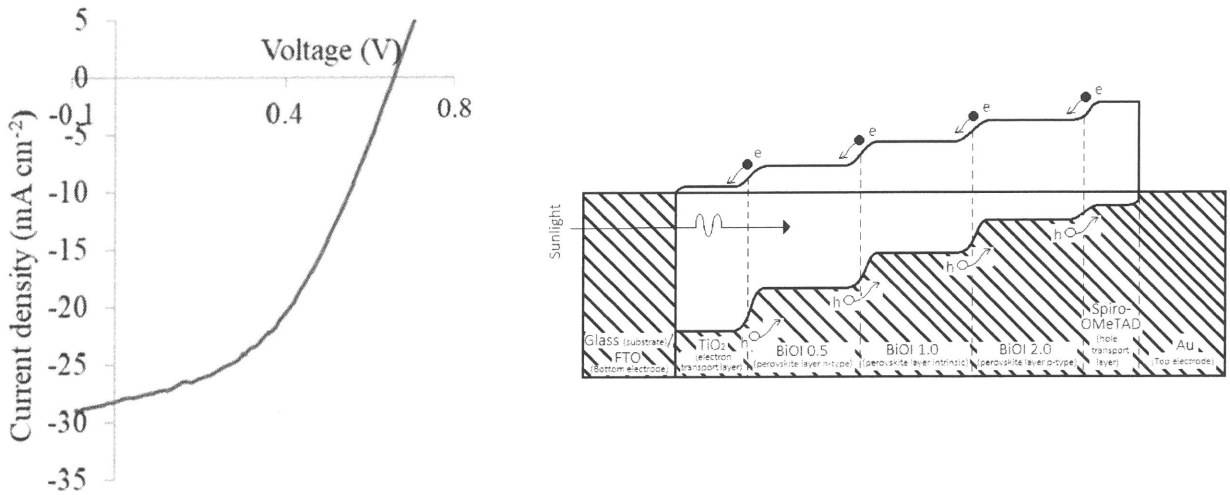

Fig. 6. J-V characteristic of graded bandgap active layers perovskite solar cell.

4. Conclusions

Graded band-gap PSCs has been fabricated by tuning the band-gap and conductivity type of bismuth halide perovskite as active layers in PSCs. Theoretically, this configuration could improve better performance from the previous (single active layer) design since with this wide band-gap layer at the front, the electromagnetic (EM) spectrum of light (photons) would be effectively absorbed and improve the seperation of the charge carriers to the external circuit. From this work, it is evident that the device with graded band-gap structure exhibit high performance (J_{sc}, V_{oc} and efficiency) compared to the device with single layer. Therefore, the findings suggested that the PSCs device can be improved through device architecture of active layer, where this design has maximized the absorption of solar radiation as well as minimized thermalization effect in the solar cell device.

Acknowledgement

This research was funded by a grant from Ministry of Higher Education of Malaysia (FRGS Grant FRGS/1/2019/STG07/UPNM/02/3).

References

[1] Xinhui Luo, Xiao Liu, Liyuan Han. "Lead-free perovskite solar cells, what's next?" *Next Energy*, 1, no. 1 (2023): 100011. https://doi.org/10.1016/j.nxener.2023.100011

[2] Tress, W and Sirtl, M. T. "$Cs_2AgBiBr_6$ double perovskites as lead-free alternatives for perovskite solar cells" *Solar RRL*, 6 (2022): 2100770. https://doi.org/10.1002/solr.202100770

[3] Ghosh, S., Shankar, H and Kar, P. "Recent developments of lead-free halide double perovskites: a new superstar in the optoelectronic field" *Mater. Adv.*, 3 (2022): 3742-3765. https://doi.org/10.1039/d2ma00071g

[4] Tahmida N. Huq, Lana C. Lee, Lissa Eyre, Weiwei Li, Robert A. Jagt, Chaewon Kim, Sarah Fearn, Felix Deschler, Judith L. MacManus-Driscoll, Robert L. Z. Hoye "Electronic Structure and Optoelectronic Properties of Bismuth Oxyiodide Robust against Percent-Level Iodine-, Oxygen-, and Bismuth-Related Surface Defects" *Advanced Functional Materials*, 30:13, (2020): 1909983. https://doi.org/10.1002/adfm.201909983

[5] Terry Chien-Jen Yang, Peter Fiala, Quentin Jeangros, Christophe Ballif. "High-Bandgap Perovskite Materials for Multijunction Solar Cells" *Joule*, 2, no. 8 (2018): 1421-1436. https://doi.org/10.1016/j.joule.2018.05.008.

[6] Ergen, O., Gilbert, S., Pham, T., Turner, S., Tan, M., Worsley, M., & Zettl, A. (2017/05//). Graded bandgap perovskite solar cells. *Nature Materials, 16*, no. 5 (2017): 522-525. https://doi.org/10.1038/nmat4795

[7] Xiao, X. and Zhang, W. D. "Facile synthesis of nanostructured BiOI microspheres with high visible light-induced photocatalytic activity" *Journal of Materials Chemistry*, 20(28) (2020): 5866-5870. https://doi.org/10.1039/C0JM00333F

[8] Kasap, S. and Capper, P. eds., 2017. *Springer handbook of electronic and photonic materials*. Springer.

[9] N. C. Miller and M. Bernechea, "Research Update: Bismuth based materials for photovoltaics" *APL Materials*, 6, 084503 (2018). https://doi.org/10.1063/1.5026542

[10] Abdul-Manaf, N. A., Azmi, A. H., Fauzi, F. and Mohamed, N.S. "The effects of micro and macro structure on electronic properties of bismuth oxyiodide thin films" *Material Research Express*, 8 (2021):096401 https://doi.org/10.1088/2053-1591/ac20f7

[11] Kim, Hui-Seon, Anders Hagfeldt, and Nam-Gyu Park. "Morphological and compositional progress in halide perovskite solar cells." *Chemical communications* 55, no. 9 (2019): 1192-1200. https://doi.org/10.1039/C8CC08653B

[12] Eguchi, R., Yamamuro, H. and Takashiri, M., "Enhanced thermoelectric properties of electrodeposited Bi2Te3 thin films using TiN diffusion barrier layer on a stainless-steel substrate and thermal annealing" *Thin Solid Films*, 714 (2020):138356. https://doi.org/10.1016/j.tsf.2020.138356

[13] Delhaise, André M., and Doug D. Perovic. "Study of solid-state diffusion of Bi in polycrystalline Sn using electron probe microanalysis." *Journal of electronic materials* 47 (2018): 2057-2065. https://doi.org/10.1016/j.tsf.2020.138356

[14] Matiur, R.M., Abuelwafa, A.A., Putri, A.A. *et al.* "Annealing effects on structural and photovoltaic properties of the dip-SILAR-prepared bismuth oxyhalides (BiOI, $Bi_7O_9I_3$, Bi_5O_7I) films." *SN Appl. Sci.* 3 (2021):138 https://doi.org/10.1007/s42452-021-04153-y

[15] Alla, Mohamed, Santosh Bimli, Vishesh Manjunath, Manopriya Samtham, Abhishek Kasaudhan, Ekta Choudhary, Mustapha Rouchdi, and Fares Boubker. "Towards Lead-Free All-Inorganic Perovskite Solar Cell with Theoretical Efficiency Approaching 23%." Materials Technology 37, no. 14 (2022):2963–69. https://doi.org/10.1080/10667857.2022.2091195.

[16] Bhandari S., Mondal D., Nataraj S.K., Balakrishna R.G. Biomolecule-derived quantum dots for sustainable optoelectronics. Nanoscale Adv. 2019;1:913–936. https://doi.org/10.1039/C8NA00332G.

[17] Kawano, Y., Chantana, J., Nishimura, T., Abdurashid, M. and Takashi, M. "Bismuth-doped Cu(In,Ga)Se2 solar cell on flexible stainless steel substrate: Examination of bismuth-doping effectiveness under different substrate temperatures on photovoltaic performances" Solar Energy, 208 (2020):20-30 https://doi.org/10.1016/j.solener.2020.07.076.

[18] Sun, H., Kaimo, D., Jie, X. and Li, L. "Graded Bandgap Perovskite with Intrinsic n–p Homojunction Expands Photon Harvesting Range and Enables All Transport Layer-Free Perovskite Solar Cells" *Advanced Energy Materials* (2020) https://doi.org/10. 10.1002/aenm.201903347

[19] Ojo, A. A., Cranton, W. M., Dharmadasa, I.M. "Next generation multilayer graded bandgap solar cells". New York: Springer International Publishing; 2019.

[20] Dharmadasa, I. M. "Advances in thin-film solar cells" Jenny Stanford Publishing; 2018 Sep 5. https://doi.org/10.1201/9780429020841